



Article

# $\beta,\beta$ -Isomer of Open-Wells–Dawson Polyoxometalate Containing a Tetra-Iron(III) Hydroxide Cluster: $[\{\text{Fe}_4(\text{H}_2\text{O})(\text{OH})_5\}(\beta,\beta\text{-Si}_2\text{W}_{18}\text{O}_{66})]^{9-}$

Satoshi Matsunaga, Eriko Miyamae, Yusuke Inoue and Kenji Nomiya \*

Department of Chemistry, Faculty of Science, Kanagawa University, Hiratsuka, Kanagawa 259-1293, Japan; matsunaga@kanagawa-u.ac.jp (S.M.); miyamae.527@gmail.com (E.M.); r201470042gl@jindai.jp (Y.I.)

\* Correspondence: nomiya@kanagawa-u.ac.jp; Tel.: +81-463-59-4111

Academic Editor: Duncan H. Gregory

Received: 15 April 2016; Accepted: 9 May 2016; Published: 17 May 2016

**Abstract:** The  $\beta,\beta$ -isomer of open-Wells–Dawson polyoxometalate (POM) containing a tetra-iron(III) cluster,  $\text{K}_9[\{\text{Fe}_4(\text{H}_2\text{O})(\text{OH})_5\}(\beta,\beta\text{-Si}_2\text{W}_{18}\text{O}_{66})] \cdot 17\text{H}_2\text{O}$  (potassium salt of  $\beta,\beta\text{-Fe}_4\text{-open}$ ), was synthesized by reacting  $\text{Na}_9\text{H}[\text{A-}\beta\text{-SiW}_9\text{O}_{34}] \cdot 23\text{H}_2\text{O}$  with  $\text{FeCl}_3 \cdot 6\text{H}_2\text{O}$  at pH 3, and characterized by X-ray crystallography, FTIR, elemental analysis, TG/DTA, UV–Vis, and cyclic voltammetry. X-ray crystallography revealed that the  $\{\text{Fe}^{3+}_4(\text{H}_2\text{O})(\text{OH})_5\}^{7+}$  cluster was included in the open pocket of the  $\beta,\beta$ -type open-Wells–Dawson polyanion  $[\beta,\beta\text{-Si}_2\text{W}_{18}\text{O}_{66}]^{16-}$  formed by the fusion of two trilacunary  $\beta$ -Keggin POMs,  $[\text{A-}\beta\text{-SiW}_9\text{O}_{34}]^{10-}$ , via two W–O–W bonds. The  $\beta,\beta$ -open-Wells–Dawson polyanion corresponds to an open structure of the standard  $\gamma$ -Wells–Dawson POM.  $\beta,\beta\text{-Fe}_4\text{-open}$  is the first example of the compound containing a geometrical isomer of  $\alpha,\alpha$ -open-Wells–Dawson structural POM.

**Keywords:** polyoxometalates; open-Wells–Dawson structural POM; iron; geometrical isomer

## 1. Introduction

Polyoxometalates (POMs) are discrete metal oxide clusters that are of interest as soluble metal oxides, with applications in catalysis, medicine, and materials science [1–13]. Recently, the open-Wells–Dawson POMs have been an emerging class of POMs [14–28]. The standard Wells–Dawson structural POM is regarded as an assembly of two trilacunary Keggin POMs via six W–O–W bonds. In 2014, Mizuno *et al.* reported the synthesis of a standard Wells–Dawson structural POM with a highly charged guest  $\text{SiO}_4^{4-}$ ,  $\text{TBA}_8[\alpha\text{-Si}_2\text{W}_{18}\text{O}_{62}] \cdot 3\text{H}_2\text{O}$ , by dimerization of a trilacunary Keggin POM,  $[\alpha\text{-SiW}_9\text{O}_{34}]^{10-}$ , in an organic solvent [29]. However, in aqueous media, the electrostatic repulsion induced by the highly charged guest  $\text{XO}_4^{4-}$  ( $\text{X} = \text{Si}, \text{Ge}$ ) inhibits the assembly of the standard Wells–Dawson structure [30]. Therefore, the two trilacunary Keggin units with  $\text{XO}_4^{4-}$  ( $\text{X} = \text{Si}, \text{Ge}$ ) are linked by two W–O–W bonds, forming open-Wells–Dawson structural POMs. The open pocket of these POMs can accommodate up to six metals. Thus, these compounds constitute a promising platform for the development of metal-substituted POM-based materials and catalysts. To date, many compounds with various metal ions in their open pocket have been reported. For example,  $\text{V}^{5+}$  [19],  $\text{Mn}^{2+}$  [16,21],  $\text{Fe}^{3+}$  [19],  $\text{Co}^{2+}$  [14,16,20,21,25,27],  $\text{Ni}^{2+}$  [16,21,24,27],  $\text{Cu}^{2+}$  [15–17],  $\text{Zn}^{2+}$  [23],  $\text{Al}^{3+}$  [28],  $\text{Ga}^{3+}$  [28], and lanthanoid ( $\text{Eu}^{3+}$ ,  $\text{Gd}^{3+}$ ,  $\text{Tb}^{3+}$ ,  $\text{Dy}^{3+}$ ,  $\text{Ho}^{3+}$ ) [22,26].

The standard Wells–Dawson structural POM is one of the most deeply studied POMs. Baker and Figgis predicted the existence of six possible structural isomers of the Wells–Dawson POM ( $\alpha$ ,  $\beta$ ,  $\gamma$ ,  $\alpha^*$ ,  $\beta^*$ ,  $\gamma^*$ ) [31]. So far, only the  $\alpha$ -,  $\beta$ -,  $\gamma$ -, and  $\gamma^*$ - isomers have been experimentally confirmed [32–37]. The  $\alpha$ -Wells–Dawson POM has  $D_{3h}$  symmetry (Figure 1, upper left). The  $\beta$ - and  $\gamma$ -Wells–Dawson isomers exhibit  $C_{3v}$  and  $D_{3h}$  symmetries, respectively, and are derived from the  $\alpha$ -Wells–Dawson

isomer by a  $60^\circ$  rotation of one ( $\beta$ -isomer) or two ( $\gamma$ -isomer)  $\{M_3O_{13}\}$  caps about the three-fold axis of the  $\alpha$ -Wells–Dawson isomer (Figure 1, upper middle and right). Likewise, the  $\alpha^*$ -,  $\beta^*$ -, and  $\gamma^*$ -Wells–Dawson isomers are derived from the  $\alpha$ -,  $\beta$ -, and  $\gamma$ -isomer by a  $60^\circ$  rotation of half  $\{XM_9\}$  units.

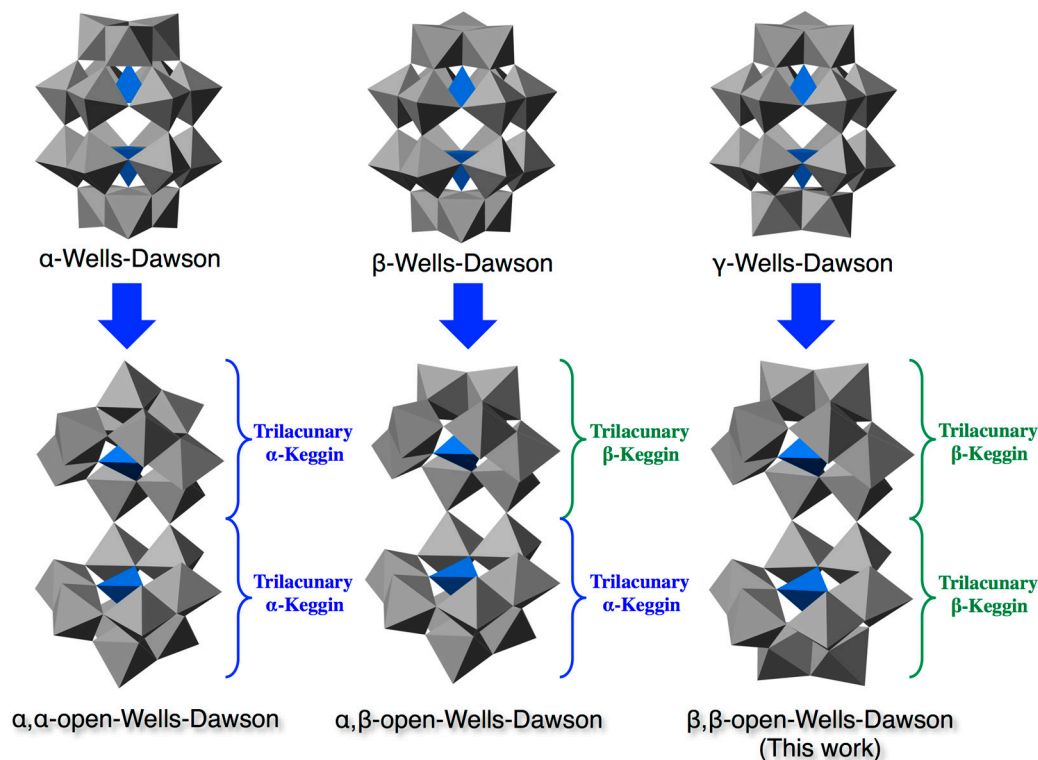


**Figure 1.** The isomers of the usual Wells–Dawson structural POMs and the open-Wells–Dawson POMs. Color code:  $XO_4$ , blue;  $WO_6$ , gray.

On the basis of the analogy with the standard Wells–Dawson isomers, the isomers of the open-Wells–Dawson POMs are possible. The well-known  $\alpha, \alpha$ -open-Wells–Dawson POM [ $\alpha, \alpha$ - $X_2W_{18}O_{66}$ ] $^{16-}$ , built from two trilacunary  $\alpha$ -Keggin units [ $A$ - $\alpha$ - $XW_9O_{34}$ ] $^{10-}$  by two W–O–W bonds, corresponds to an open structure of the conventional  $\alpha$ -Wells–Dawson POM (Figure 1, lower left). A similar assembly of two trilacunary  $\beta$ -Keggin units prompts the  $\beta, \beta$ -open-Wells–Dawson isomer, which is viewed as an open structure of the  $\gamma$ -Wells–Dawson POM (Figure 1, lower right). Likewise, an assembly of the trilacunary  $\alpha$ - and  $\beta$ -Keggin POMs leads to the  $\alpha, \beta$ -open-Wells–Dawson isomer corresponding to an open structure of the  $\beta$ -Wells–Dawson POM. However, only the  $\alpha, \alpha$ -isomer of the open-Wells–Dawson structural POM has been reported so far.

Herein, we report the synthesis of the  $\beta, \beta$ -isomer of the open-Wells–Dawson POM containing a tetra-iron(III) cluster,  $K_9[\{Fe_4(H_2O)(OH)_5\}(\beta, \beta-Si_2W_{18}O_{66})] \cdot 17H_2O$  (potassium salt of  $\beta, \beta$ - $Fe_4$ -open) and its characterization by X-ray crystallography, FTIR, elemental analysis, TG/DTA, UV–Vis, and cyclic voltammetry. The  $\beta, \beta$ - $Fe_4$ -open is the first example of the compound containing a geometrical isomer of the  $\alpha, \alpha$ -open-Wells–Dawson structural POM.

## 2. Results and Discussion

### 2.1. Synthesis and Characterization

The potassium salts of  $\beta, \beta$ - $Fe_4$ -open,  $K_9[\{Fe_4(H_2O)(OH)_5\}(\beta, \beta-Si_2W_{18}O_{66})] \cdot 17H_2O$ , were prepared by the reaction of the separately prepared  $Na_9H[A-\beta-SiW_9O_{34}] \cdot 23H_2O$  with  $FeCl_3 \cdot 6H_2O$  in a 1:2 molar ratio at pH 3, followed by stirring the solution at  $80^\circ C$  for 30 min. The  $\beta, \beta$ -type

open-Wells–Dawson POM containing a tetra-iron(III) cluster was obtained as crystalline sample with 22.2% yield.

Equation (1) represents the formation of the polyoxoanion  $[\{\text{Fe}_4(\text{H}_2\text{O})(\text{OH})_5\}(\beta,\beta\text{-Si}_2\text{W}_{18}\text{O}_{66})]^{9-}$ .



In the case of the  $\alpha,\alpha$ -analogue, *i.e.*,  $\text{K}_2\text{Na}_8[\{\text{Fe}_4(\text{OH})_6\}(\text{Si}_2\text{W}_{18}\text{O}_{66})] \cdot 44\text{H}_2\text{O}$  ( **$\alpha,\alpha\text{-Fe}_4\text{-open}$** ) [19], the  $\text{K}^+$  ions incorporating the open-Wells–Dawson POM, *i.e.*,  $\text{K}_{13}[\{\text{K}(\text{H}_2\text{O})_3\}_2\{\text{K}(\text{H}_2\text{O})_2\}(\alpha,\alpha\text{-Si}_2\text{W}_{18}\text{O}_{66})] \cdot 19\text{H}_2\text{O}$  ( **$\text{K-open}$** ), were used as a precursor, whereas the potassium salt of  **$\beta,\beta\text{-Fe}_4\text{-open}$**  was prepared from the trilacunary  $\beta$ -Keggin POM, *i.e.*,  $\text{Na}_9\text{H}[\text{A-}\beta\text{-SiW}_9\text{O}_{34}] \cdot 23\text{H}_2\text{O}$ . Both  **$\alpha,\alpha$** - and  **$\beta,\beta\text{-Fe}_4\text{-open}$**  were prepared at *ca.* pH 3. Excess  $\text{K}^+$  ions are required for the formation of the  $\alpha,\alpha$ -open-Wells–Dawson POM [25,28], indicating that  $\text{K}^+$  ions play an important role in the synthesis. In the case of the present  $\beta,\beta$ -open-Wells–Dawson POM, the addition of excess KCl was needed, indicating that  $\text{K}^+$  ions also play an important role in the formation of the  $\beta,\beta$ -open-Wells–Dawson structural POMs.

The potassium salt of  **$\beta,\beta\text{-Fe}_4\text{-open}$**  was characterized via elemental analysis. Prior to analysis, the sample was dried overnight at room temperature under a vacuum of  $10^{-3}$ – $10^{-4}$  Torr. All elements (H, Fe, K, O, Si, and W) were analyzed for a total of 99.74%, indicating that the obtained compound was highly pure. The observed data was in accordance with the calculated values for the formula constituting four water molecules, *i.e.*,  $\text{K}_9[\{\text{Fe}_4(\text{H}_2\text{O})(\text{OH})_5\}(\beta,\beta\text{-Si}_2\text{W}_{18}\text{O}_{66})] \cdot 4\text{H}_2\text{O}$  (see Experimental Section). The weight loss observed during drying was 4.23% corresponding to *ca.* 13 crystallized water molecules (calcd. 4.33%), and therefore, the sample contained a total of 17 crystallized water molecules. On the other hand, during the TG/DTA measurements carried out under atmospheric conditions (Figure S2), a weight loss of 6.10%, observed at temperatures below 500 °C, corresponded to *ca.* 18 water molecules (calcd. 5.98%). Thus, the elemental analysis and TG/DTA displayed a presence of a total of 17–18 water molecules for the sample under atmospheric conditions. The formula for the potassium salt of  **$\beta,\beta\text{-Fe}_4\text{-open}$**  presented herein is decided as  $\text{K}_9[\{\text{Fe}_4(\text{H}_2\text{O})(\text{OH})_5\}(\beta,\beta\text{-Si}_2\text{W}_{18}\text{O}_{66})] \cdot 17\text{H}_2\text{O}$  based on the results of the complete elemental analysis.

## 2.2. Molecular Structure

X-ray crystallography of  **$\beta,\beta\text{-Fe}_4\text{-open}$**  revealed that a  $\beta,\beta$ -type open-Wells–Dawson polyanion is formed by the fusion of two trilacunary  $\beta$ -Keggin POMs,  $[\text{A-}\beta\text{-SiW}_9\text{O}_{34}]^{10-}$ , via two W–O–W bonds, and the  $\{\text{Fe}^{3+}_4(\text{H}_2\text{O})(\text{OH})_5\}^{7+}$  cluster is included in the open pocket of the  $\beta,\beta$ -type open-Wells–Dawson polyanion,  $[\beta,\beta\text{-Si}_2\text{W}_{18}\text{O}_{66}]^{16-}$  (Figure 2). The structure of the  $\beta,\beta$ -open-Wells–Dawson polyanion moiety is derived by a 60° rotation of two  $\{\text{M}_3\text{O}_{13}\}$  caps of the  $\alpha,\alpha$ -type isomer, corresponding to an open structure of the  $\gamma$ -Wells–Dawson POM; it is the first example of the isomer of the  $\alpha,\alpha$ -open-Wells–Dawson POM.

The four iron(III) centers in the open pocket were arranged in a rectangular array, and were connected to the neighboring iron atoms through edge-sharing oxygen atoms (O67, O68, O69, and O70) and corner-sharing oxygen atoms (O71 and O72). Bond valence sum (BVS) calculations [38] of the oxygen atoms connected to the iron atoms suggested that four of the oxygen atoms (O67, O69, O71, and O72) are protonated, *i.e.*, they are ascribed to the hydroxide groups (the BVS values: O67, 1.106; O69, 1.157; O71, 1.170; O72, 1.255; Table S1). On the other hand, the BVS values of two inner edge-sharing oxygen atoms (O68, 0.796 and O70, 0.660; Table S1) were slightly lower than those of other oxygen atoms connected to the iron atoms. These results suggested that there is one proton between two oxygen atoms (O68 and O70), *i.e.*, the iron(III) cluster in the open pocket can be represented as  $\{\text{Fe}_4(\text{H}_2\text{O})(\text{OH})_5\}^{7+}$ . All the iron atoms were in the +3 oxidation state (the BVS values: Fe1, 2.981; Fe2, 3.030; Fe3, 3.018; Fe4, 3.148; Table S1). These results were consistent with elemental analysis of the potassium salt of  **$\beta,\beta\text{-Fe}_4\text{-open}$** . The Fe...Fe distances connected through edge-sharing oxygen atoms were 3.103(4) (Fe1–Fe3) and 3.114(4) (Fe2–Fe4) Å, and through corner-sharing oxygen atoms were

3.648(5) (Fe1–Fe2) and 3.646(5) (Fe3–Fe4). This metal ion arrangement was similar to that of previously reported  $\alpha,\alpha$ -Fe<sub>4</sub>-open [19], and  $[[M_4(OH)_6](\alpha,\alpha\text{-Si}_2W_{18}O_{66})]^{10-}$  (M = Al, Ga) [28].

The bite angle of  $\beta,\beta$ -Fe<sub>4</sub>-open was 58.736°, similar to that of  $\alpha,\alpha$ -Fe<sub>4</sub>-open (58.147°), and as for the structure around the open pocket, no clear difference was observed between the  $\alpha,\alpha$ - and  $\beta,\beta$ -Fe<sub>4</sub>-open.

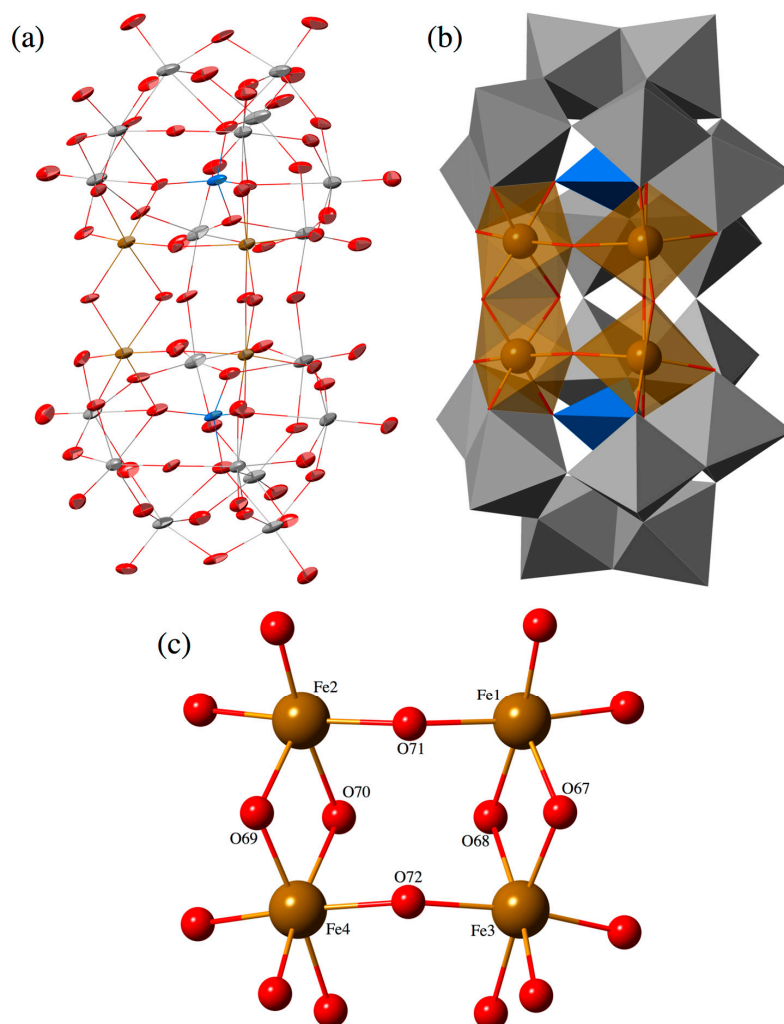


**Figure 2.** (a) Molecular structure of the polyoxoanion  $[\text{Fe}_4(\text{H}_2\text{O})(\text{OH})_5](\beta,\beta\text{-Si}_2\text{W}_{18}\text{O}_{66})^{9-}$  of potassium salt of  $\beta,\beta$ -Fe<sub>4</sub>-open; (b) its polyhedral representation; and (c) the partial structure around the Fe<sub>4</sub> center. Color code: Fe, brown; O, red; Si, blue; W, gray.

There are many interactions between the oxygen atoms of the polyanion moiety and K<sup>+</sup> in the crystal structure of  $\beta,\beta$ -Fe<sub>4</sub>-open. In particular, the terminal (O15, O16, O37, O38) oxygen atoms of the WO<sub>6</sub> polyhedra serve as a hinge between the two trilacunary Keggin units interacting with K<sup>+</sup> cations (K1) (K1-O15, 2.800(14); K1-O16, 2.689(12); K1-O37, 2.685(14); K1-O38, 2.819(14) Å; Figure 3). These interactions play an important role in the formation of the  $\beta,\beta$ -type open-Wells–Dawson structural POMs and have been previously reported for the  $\alpha,\alpha$ -open-Wells–Dawson POMs [28].

### 2.3. Absorption Spectrum

The absorption spectrum of  $\beta,\beta$ -Fe<sub>4</sub>-open in H<sub>2</sub>O is shown in Figure 4. The shoulder band due to the O to Fe<sup>3+</sup> charge transfer [39] was observed around 450 nm ( $\epsilon = 98 \text{ M}^{-1} \cdot \text{cm}^{-1}$ ). This spectrum was similar to that of  $\alpha,\alpha$ -Fe<sub>4</sub>-open (Figure S3).

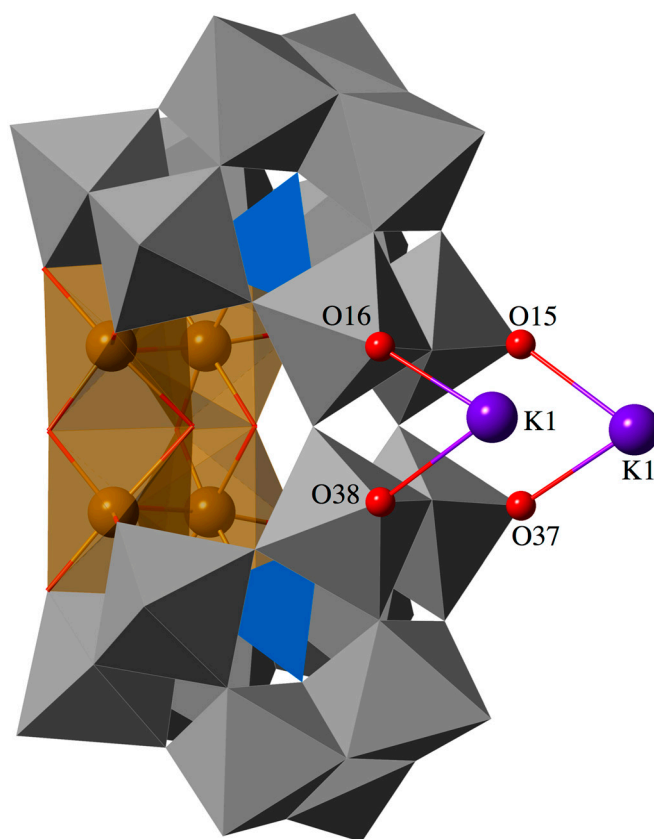


**Figure 3.** Interactions with  $K^+$  ions of the terminal oxygen atoms of the  $WO_6$  polyhedra serving as a hinge between the two trilacunary  $\beta$ -Keggin units of  $\beta,\beta\text{-Fe}_4\text{-open}$ .

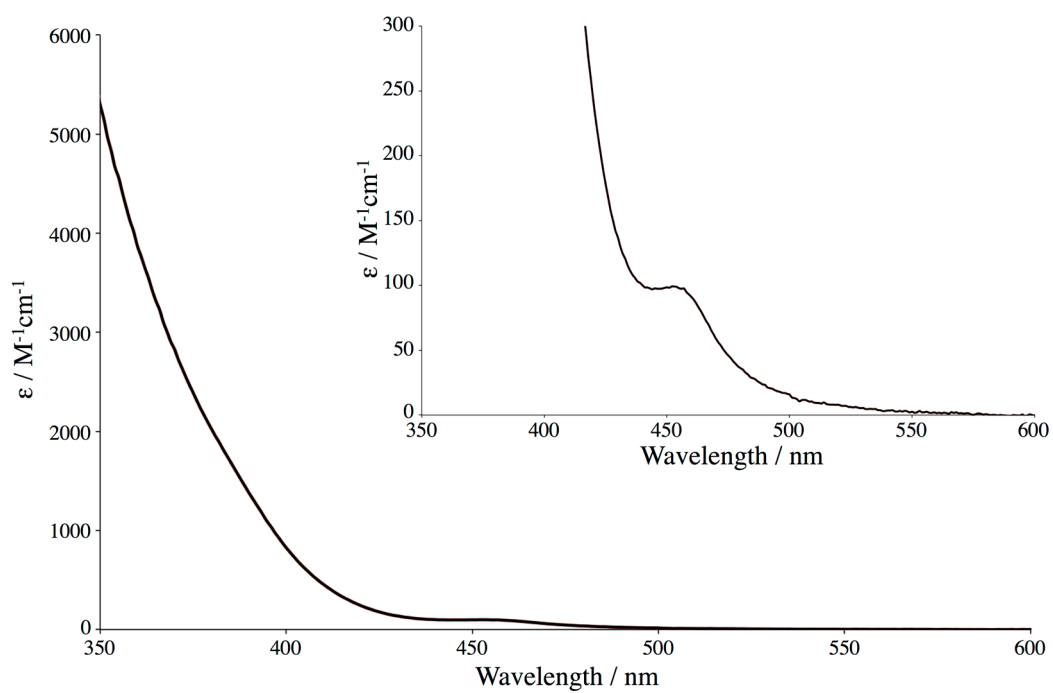


**Figure 4.** UV/Vis absorption spectrum of potassium salt of  $\beta,\beta\text{-Fe}_4\text{-open}$  in  $H_2O$ . Inset shows enlarged view.

## 2.4. Electrochemistry

The cyclic voltammogram of 0.5 mM  $\beta,\beta\text{-Fe}_4\text{-open}$  conducted in 0.5 M KOAc/HOAc buffer (pH 4.8) solution at a scan rate of  $25\text{ mV}\cdot\text{s}^{-1}$  showed three characteristic peaks at  $-0.665$ ,  $-0.794$ , and  $-0.939\text{ V}$  (*vs.* Ag/AgCl), respectively. These peaks were associated with  $\text{W}^{6+}$  centered reduction processes (Figure 5). Hill *et al.* have reported similar redox processes based on Zn-containing open-Wells–Dawson POMs [23], and noted that the second reduction wave associated with  $\text{W}^{6+}$  is a two-electron process. The cyclic voltammogram of 0.5 mM  $\alpha,\alpha\text{-Fe}_4\text{-open}$  in 0.5 M KOAc/HOAc buffer (pH 4.8) solution at a scan rate of  $25\text{ mV/s}$  was similar to that of  $\beta,\beta\text{-Fe}_4\text{-open}$  (Figure S4). However, the reduction processes of  $\alpha,\alpha\text{-Fe}_4\text{-open}$  based on  $\text{W}^{6+}$  were observed at a slightly more negative potential *i.e.*, ( $-0.704$ ,  $-0.866$ ,  $-0.936\text{ V}$  *vs.* Ag/AgCl) (Figure S4).

On the other hand, the redox waves observed at  $-0.212$  and  $0.380\text{ V}$  can be attributed to the redox processes of  $\text{Fe}^{3+}$  centers, since the Zn-containing open-Wells–Dawson POM displayed no redox waves in this region [23]. The area ratio between the second reduction wave of  $\text{W}^{6+}$  (two-electron process,  $E = -0.794\text{ V}$ ) and the reduction of  $\text{Fe}^{3+}$  ( $E = -0.212\text{ V}$ ) is *ca.* 1:2, *i.e.*, 2:4 electrons. Based on the comparison of the area ratio, the wave is likely to be the simultaneous one-electron redox of the four- $\text{Fe}^{3+}$  center.

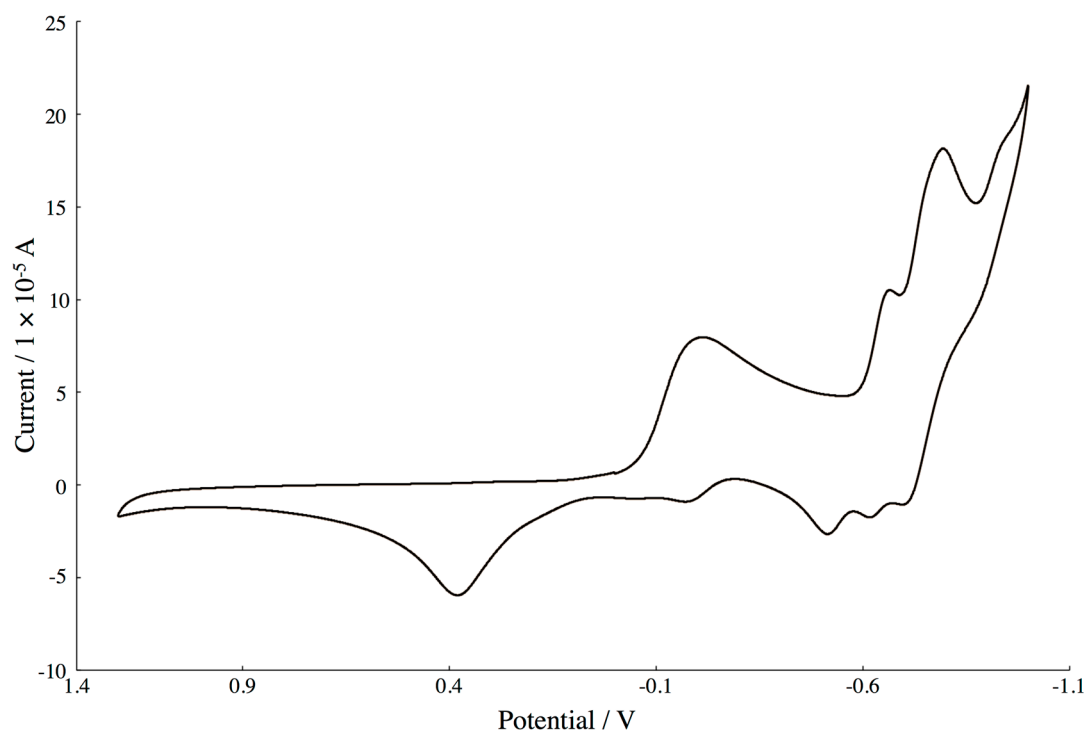


**Figure 5.** Cyclic voltammograms (CV) of 0.5 mM potassium salt of  $\beta,\beta\text{-Fe}_4\text{-open}$  in 0.5 M potassium acetate buffer, pH 4.8, scan rate  $25\text{ mV}\cdot\text{s}^{-1}$ , under  $\text{N}_2$ .

## 3. Experimental Section

### 3.1. Materials

The following reagents were used as received:  $\text{FeCl}_3\cdot 6\text{H}_2\text{O}$ , HCl, KOH, and KCl (from Wako Pure Chemical Industries, Osaka, Japan). The sodium salt of trilacunary Keggin POM, *i.e.*,  $\text{Na}_9\text{H}[\text{A-}\beta\text{-SiW}_9\text{O}_{34}]\cdot 23\text{H}_2\text{O}$ , and  $\alpha,\alpha\text{-Fe}_4\text{-open}$  were prepared according to the literature method [19,40], and identified by X-ray crystallography, TG/DTA, FT-IR, UV/Vis absorption spectra, and cyclic voltammetry.

### 3.2. Instrumentation and Analytical Procedures

Elemental analyses were carried out by Mikroanalytisches Labor Pascher (Remagen, Germany). The sample was dried overnight at room temperature under  $10^{-3}$ – $10^{-4}$  Torr before analysis. Infrared spectra were recorded on a Jasco 4100 FTIR spectrometer (Jasco, Hachioji, Japan) using KBr disks at room temperature. Thermogravimetric (TG) and differential thermal analyses (DTA) were acquired using a Rigaku Thermo Plus 2 series TG8120 instrument (Rigaku, Akishima, Japan). TG/DTA measurements were run under air with a temperature ramp of 4.0 °C/min between 20 and 500 °C. Absorption spectra in H<sub>2</sub>O were obtained on a JASCO V-630 spectrophotometer (Jasco). Cyclic voltammetry was performed with ALS/CH Instruments (BAS, Sumida-ku, Japan), a Model 610E electrochemical analyzer with a three electrode cell in 0.5 M KOAc/HOAc buffer (pH 4.8) under N<sub>2</sub> atmosphere. A glassy carbon working electrode, a Pt auxiliary electrode and a Ag/AgCl reference electrode were employed. The scan rate was 25 mV · s<sup>-1</sup>.

### 3.3. Synthesis of K<sub>9</sub>[{Fe<sub>4</sub>(H<sub>2</sub>O)(OH)<sub>5</sub>}(β,β-Si<sub>2</sub>W<sub>18</sub>O<sub>66</sub>)] · 17H<sub>2</sub>O (Potassium Salt of β,β-Fe<sub>4</sub>-Open)

Na<sub>9</sub>H[A-β-SiW<sub>9</sub>O<sub>34</sub>] · 23H<sub>2</sub>O (1.00 g, 0.351 mmol) was suspended in 50 mL of water. The pH was adjusted to 3.0 using 1.0 M HCl<sub>aq</sub>, and 1.0 mL of saturated KCl<sub>aq</sub> was added to the solution. Upon addition of FeCl<sub>3</sub> · 6H<sub>2</sub>O (0.190 g, 0.703 mmol) to the solution, the pH dropped to 1.57. Subsequently, the pH was adjusted to 3.0 using 1.0 M KOH<sub>aq</sub>. Thereafter, the solution was heated to 80 °C for 30 min and the pH was re-adjusted to 3.0 using 1.0 M KOH<sub>aq</sub>. The resulting solution was left to stand undisturbed at room temperature for one week. The resulting yellow plate crystals were collected on a membrane filter (JG 0.2 μm), and dried *in vacuo* for 2 h to obtain a yield of 0.211 g (0.0390 mmol, 22.2% based on Na<sub>9</sub>H[A-β-SiW<sub>9</sub>O<sub>34</sub>] · 23H<sub>2</sub>O).

The crystalline sample was soluble in water, but insoluble in organic solvents such as methanol, ethanol, and diethyl ether. Complete elemental analysis (%) calcd. for H<sub>15</sub>Fe<sub>4</sub>K<sub>9</sub>O<sub>76</sub>Si<sub>2</sub>W<sub>18</sub> or K<sub>9</sub>[{Fe<sub>4</sub>(H<sub>2</sub>O)(OH)<sub>5</sub>}(β,β-Si<sub>2</sub>W<sub>18</sub>O<sub>66</sub>)] · 4H<sub>2</sub>O: H, 0.29; Fe, 4.32; K, 6.80; O, 23.51; Si, 1.09; W, 63.99. Found: H, 0.29; Fe, 4.25; K, 6.57; O, 23.6; Si, 1.23; W, 63.8; total ~99.74%. A weight loss of 4.23% (solvated water) was observed during overnight drying at room temperature, at  $10^{-3}$ – $10^{-4}$  Torr before analysis, suggesting the presence of 13 water molecules (calcd. 4.33%). TG/DTA under atmospheric conditions: a weight loss of 6.10% was observed below 500 °C; calc. 5.98% for x = 18 in K<sub>9</sub>[{Fe<sub>4</sub>(H<sub>2</sub>O)(OH)<sub>5</sub>}(β,β-Si<sub>2</sub>W<sub>18</sub>O<sub>66</sub>)] · xH<sub>2</sub>O. IR (KBr, cm<sup>-1</sup>): 1615 (w), 1090 (w), 1008 (w), 962 (s), 906 (vs), 879 (vs), 810 (vs), 761 (vs), 716 (s), 643 (m), 520 (w), 483 (w), 407 (w).

### 3.4. X-ray Crystallography

For the potassium salt of β,β-Fe<sub>4</sub>-open, a single crystal with dimensions of 0.11 × 0.08 × 0.07 mm<sup>3</sup> was surrounded by liquid paraffin (Paratone-N) and analyzed at 100(2) K. Measurement was performed using a Bruker SMART APEX CCD diffractometer. The structure was solved by direct methods (SHELXS-97), followed by difference Fourier calculations and refinement by a full-matrix least-squares procedure on F<sup>2</sup> (program SHELXL-97) [41].

Crystal data: triclinic, space group P-1, a = 12.560(2), b = 19.013(3), c = 20.359(4) Å, α = 92.925(3), β = 98.002(3), γ = 93.086(3)°, V = 4799.1(15) Å<sup>3</sup>, Z = 2, D<sub>calcd</sub> = 3.694 g · cm<sup>-3</sup>, μ(Mo-Kα) = 22.371 mm<sup>-1</sup>. R<sub>1</sub> (I > 2.00σ(I)) = 0.0605, R (all data) = 0.0751, wR<sub>2</sub> (all data) = 0.1642, GOF = 1.032. Most atoms in the main part of the structure were refined anisotropically, while the rest (as crystallization solvents) were refined isotropically, because of the presence of disorder. The composition and formula of the POM, containing countercations and crystalline water molecules, were determined by the complete elemental and TG analyses. Similar to other structural investigations of crystals of highly hydrated large polyoxometalate complexes, it was not possible to locate every countercation and hydrated water molecule, due to the extensive disorder of the cations and crystalline water molecules. Further details of the crystal structure investigations may be obtained from the Fachinformationszentrum Karlsruhe, 76344 Eggenstein-Leopoldshafen, Germany (Fax: +49-7247-808-666; E-Mail: crysdata@fiz-karlsruhe.de,

[http://www.fiz-karlsruhe.de/request\\_for\\_deposited\\_data.html?&L=1](http://www.fiz-karlsruhe.de/request_for_deposited_data.html?&L=1)) on quoting the depository number CSD-431049 (Identification code; em1-6-3c).

#### 4. Conclusions

In summary, we prepared a  $\beta,\beta$ -isomer of open-Wells–Dawson POM containing a tetra-iron(III) cluster,  $K_9[\{Fe_4(H_2O)(OH)_5\}(\beta,\beta-Si_2W_{18}O_{66})] \cdot 17H_2O$  (potassium salt of  $\beta,\beta$ -Fe<sub>4</sub>-open), by reacting trilacunary  $\beta$ -Keggin POM,  $Na_9H[A-\beta-SiW_9O_{34}] \cdot 23H_2O$ , with  $FeCl_3 \cdot 6H_2O$ . This compound is the first example containing the isomer of  $\alpha,\alpha$ -open-Wells–Dawson structural POM. Studies on the  $\alpha,\beta$ -isomers of open-Wells–Dawson POMs, regarded as an open structure of the standard  $\beta$ -Wells–Dawson POM, are in progress.

**Supplementary Materials:** The following are available online at [www.mdpi.com/2304-6740/4/2/15/s1](http://www.mdpi.com/2304-6740/4/2/15/s1), Table S1: Bond valence sum (BVS) calculations of Fe and O atoms of the  $\{Fe_4(H_2O)(OH)_5\}$  cluster moieties of  $\beta,\beta$ -Fe<sub>4</sub>-open; Figure S1: FT-IR spectrum of potassium salt of  $\beta,\beta$ -Fe<sub>4</sub>-open (KBr disk); Figure S2: TG/DTA data of potassium salt of  $\beta,\beta$ -Fe<sub>4</sub>-open; Figure S3: UV/Vis absorption spectra of  $\alpha,\alpha$ - and  $\beta,\beta$ -Fe<sub>4</sub>-open in H<sub>2</sub>O; Figure S4: Cyclic voltammograms (CV) of 0.5 mM potassium salt of  $\alpha,\alpha$ - and  $\beta,\beta$ -Fe<sub>4</sub>-open in 0.5 M potassium acetate buffer, pH 4.8, scan rate 25 mV · s<sup>-1</sup>, under N<sub>2</sub>; checkCIF/PLATON report.

**Acknowledgments:** This study was supported by the Strategic Research Base Development Program for Private Universities of the Ministry of Education, Culture, Sports, Science and Technology of Japan, and also by a grant from Research Institute for Integrated Science, Kanagawa University (RIIS201505).

**Author Contributions:** Satoshi Matsunaga and Kenji Nomiya conceived and designed the experiments, and wrote the paper; Eriko Miyamae and Yusuke Inoue synthesized and characterized the compound.

**Conflicts of Interest:** The authors declare no conflict of interest.

#### Abbreviations

The following abbreviations are used in this manuscript:

POM	Polyoxometalate
TG/DTA	Thermogravimetric/differential thermal analyses
BVS	Bond valence sum

#### References

1. Pope, M.T.; Müller, A. Polyoxometalate chemistry: An old field with new dimensions in several disciplines. *Angew. Chem. Int. Ed.* **1991**, *30*, 34–48. [[CrossRef](#)]
2. Pope, M.T. *Heteropoly and Isopolyoxometalates*; Springer-Verlag: New York, NY, USA, 1983.
3. Hill, C.L.; Prosser-McCartha, C.M. Homogeneous catalysis by transition metal oxygen anion clusters. *Coord. Chem. Rev.* **1995**, *143*, 407–455. [[CrossRef](#)]
4. Neumann, R. Polyoxometalate complexes in organic oxidation chemistry. *Prog. Inorg. Chem.* **1998**, *47*, 317–370.
5. Proust, A.; Thouvenot, R.; Gouzerh, P. Functionalization of polyoxometalates: Towards advanced applications in catalysis and materials science. *Chem. Commun.* **2008**, 1837–1852. [[CrossRef](#)] [[PubMed](#)]
6. Hasenknopf, B.; Micoine, K.; Lacôte, E.; Thorimbert, S.; Malacria, M.; Thouvenot, R. Chirality in polyoxometalate chemistry. *Eur. J. Inorg. Chem.* **2008**, 5001–5013. [[CrossRef](#)]
7. Long, D.-L.; Tsunashima, R.; Cronin, L. Polyoxometalates: Building blocks for functional nanoscale systems. *Angew. Chem. Int. Ed.* **2010**, *49*, 1736–1758. [[CrossRef](#)] [[PubMed](#)]
8. Nomiya, K.; Sakai, Y.; Matsunaga, S. Chemistry of group IV metal ion-containing polyoxometalates. *Eur. J. Inorg. Chem.* **2011**, 179–196. [[CrossRef](#)]
9. Izarova, N.V.; Pope, M.T.; Kortz, U. Noble metals in polyoxometalates. *Angew. Chem. Int. Ed.* **2012**, *51*, 9492–9510. [[CrossRef](#)] [[PubMed](#)]
10. Song, Y.-F.; Tsunashima, R. Recent advances on polyoxometalate-based molecular and composite materials. *Chem. Soc. Rev.* **2012**, *41*, 7384–7402. [[CrossRef](#)] [[PubMed](#)]
11. Bijelic, A.; Rompel, A. The use of polyoxometalates in protein crystallography—An attempt to widen a well-known bottleneck. *Coord. Chem. Rev.* **2015**, *299*, 22–38. [[CrossRef](#)] [[PubMed](#)]



12. Wang, S.-S.; Yang, G.-Y. Recent advances in polyoxometalate-catalyzed reactions. *Chem. Rev.* **2015**, *115*, 4893–4962. [[CrossRef](#)] [[PubMed](#)]
13. Blazevic, A.; Rompel, A. The Anderson–Evans polyoxometalate: From inorganic building blocks via hybrid organic–inorganic structures to tomorrows “Bio-POM”. *Coord. Chem. Rev.* **2016**, *307*, 42–64. [[CrossRef](#)]
14. Laronze, N.; Marrot, J.; Hervé, G. Synthesis, molecular structure and chemical properties of a new tungstosilicate with an open Wells–Dawson structure,  $\alpha$ -[Si<sub>2</sub>W<sub>18</sub>O<sub>66</sub>]<sup>16-</sup>. *Chem. Commun.* **2003**, 2360–2361. [[CrossRef](#)]
15. Bi, L.-H.; Kortz, U. Synthesis and structure of the pentacopper(II) substituted tungstosilicate [Cu<sub>5</sub>(OH)<sub>4</sub>(H<sub>2</sub>O)<sub>2</sub>(A- $\alpha$ -SiW<sub>9</sub>O<sub>33</sub>)<sub>2</sub>]<sup>10-</sup>. *Inorg. Chem.* **2004**, *43*, 7961–7962. [[CrossRef](#)] [[PubMed](#)]
16. Leclerc-Laronze, N.; Marrot, J.; Hervé, G. Cation-directed synthesis of tungstosilicates. 2. Synthesis, structure, and characterization of the open Wells–Dawson anion  $\alpha$ -[K(H<sub>2</sub>O)<sub>2</sub>](Si<sub>2</sub>W<sub>18</sub>O<sub>66</sub>)<sup>15-</sup> and its transition-metal derivatives [[M(H<sub>2</sub>O)]( $\mu$ -H<sub>2</sub>O)<sub>2</sub>K(Si<sub>2</sub>W<sub>18</sub>O<sub>66</sub>)]<sup>13-</sup> and [[M(H<sub>2</sub>O)]( $\mu$ -H<sub>2</sub>O)<sub>2</sub>K{M(H<sub>2</sub>O)<sub>4</sub>}(Si<sub>2</sub>W<sub>18</sub>O<sub>66</sub>)]<sup>11-</sup>. *Inorg. Chem.* **2005**, *44*, 1275–1281. [[PubMed](#)]
17. Nellutla, S.; Tol, J.V.; Dalal, N.S.; Bi, L.-H.; Kortz, U.; Keita, B.; Nadjo, L.; Khitrov, G.A.; Marshall, A.G. Magnetism, electron paramagnetic resonance, electrochemistry, and mass spectrometry of the pentacopper(II)-substituted tungstosilicate [Cu<sub>5</sub>(OH)<sub>4</sub>(H<sub>2</sub>O)<sub>2</sub>(A- $\alpha$ -SiW<sub>9</sub>O<sub>33</sub>)<sub>2</sub>]<sup>10-</sup>, A model five-spin frustrated cluster. *Inorg. Chem.* **2005**, *44*, 9795–9806. [[CrossRef](#)] [[PubMed](#)]
18. Leclerc-Laronze, N.; Haouas, M.; Marrot, J.; Taulelle, F.; Hervé, G. Step-by-step assembly of trivacant tungstosilicates: Synthesis and characterization of tetrameric anions. *Angew. Chem. Int. Ed.* **2006**, *45*, 139–142. [[CrossRef](#)] [[PubMed](#)]
19. Leclerc-Laronze, N.; Marrot, J.; Hervé, G. Dinuclear vanadium and tetranuclear iron complexes obtained with the open Wells–Dawson [Si<sub>2</sub>W<sub>18</sub>O<sub>66</sub>]<sup>16-</sup> tungstosilicate. *C. R. Chim.* **2006**, *9*, 1467–1471. [[CrossRef](#)]
20. Sun, C.-Y.; Liu, S.-X.; Wang, C.-L.; Xie, L.-H.; Zhang, C.-D.; Gao, B.; Su, Z.-M.; Jia, H.-Q. Synthesis, structure and characterization of a new cobalt-containing germanotungstate with open Wells–Dawson structure: K<sub>13</sub>[{Co(H<sub>2</sub>O)}( $\mu$ -H<sub>2</sub>O)<sub>2</sub>K(Ge<sub>2</sub>W<sub>18</sub>O<sub>66</sub>)]. *J. Mol. Struct.* **2006**, *785*, 170–175. [[CrossRef](#)]
21. Wang, C.-L.; Liu, S.-X.; Sun, C.-Y.; Xie, L.-H.; Ren, Y.-H.; Liang, D.-D.; Cheng, H.-Y. Bimetals substituted germanotungstate complexes with open Wells–Dawson structure: Synthesis, structure, and electrochemical behavior of [{M(H<sub>2</sub>O)}( $\mu$ -H<sub>2</sub>O)<sub>2</sub>K{M(H<sub>2</sub>O)<sub>4</sub>}(Ge<sub>2</sub>W<sub>18</sub>O<sub>66</sub>)]<sup>11-</sup> (M = Co, Ni, Mn). *J. Mol. Struct.* **2007**, *841*, 88–95. [[CrossRef](#)]
22. Ni, L.; Hussain, F.; Spingler, B.; Weyeneth, S.; Patzke, G.R. Lanthanoid-containing open Wells–Dawson silicotungstates: Synthesis, crystal structures, and properties. *Inorg. Chem.* **2011**, *50*, 4944–4955. [[CrossRef](#)] [[PubMed](#)]
23. Zhu, G.; Geletii, Y.V.; Zhao, C.; Musaev, D.G.; Song, J.; Hill, C.L. A dodecanuclear Zn cluster sandwiched by polyoxometalate ligands. *Dalton Trans.* **2012**, *41*, 9908–9913. [[CrossRef](#)] [[PubMed](#)]
24. Zhu, G.; Glass, E.N.; Zhao, C.; Lv, H.; Vickers, J.W.; Geletii, Y.V.; Musaev, D.G.; Song, J.; Hill, C.L. A nickel containing polyoxometalate water oxidation catalyst. *Dalton Trans.* **2012**, *41*, 13043–13049. [[CrossRef](#)] [[PubMed](#)]
25. Zhu, G.; Geletii, Y.V.; Song, J.; Zhao, C.; Glass, E.N.; Bacsá, J.; Hill, C.L. Di- and tri-cobalt silicotungstates: Synthesis, characterization, and stability studies. *Inorg. Chem.* **2013**, *52*, 1018–1024. [[CrossRef](#)] [[PubMed](#)]
26. Ni, L.; Spingler, B.; Weyeneth, S.; Patzke, G.R. Trilacunary Keggin-type POMs as versatile building blocks for lanthanoid silicotungstates. *Eur. J. Inorg. Chem.* **2013**, 1681–1692. [[CrossRef](#)]
27. Guo, J.; Zhang, D.; Chen, L.; Song, Y.; Zhu, D.; Xu, Y. Syntheses, structures and magnetic properties of two unprecedented hybrid compounds constructed from open Wells–Dawson anions and high-nuclear transition metal clusters. *Dalton Trans.* **2013**, *42*, 8454–8459. [[CrossRef](#)] [[PubMed](#)]
28. Matsunaga, S.; Inoue, Y.; Otaki, T.; Osada, H.; Nomiya, K. Aluminum- and Gallium-Containing Open-Dawson Polyoxometalates. *Z. Anorg. Allg. Chem.* **2016**, *642*, 539–545. [[CrossRef](#)]
29. Minato, T.; Suzuki, K.; Kamata, K.; Mizuno, N. Synthesis of  $\alpha$ -Dawson-type silicotungstate [ $\alpha$ -Si<sub>2</sub>W<sub>18</sub>O<sub>62</sub>]<sup>8-</sup> and protonation and deprotonation inside the aperture through intramolecular hydrogen bonds. *Chem. Eur. J.* **2014**, *20*, 5946–5952. [[CrossRef](#)] [[PubMed](#)]
30. Zhang, F.-Q.; Guan, W.; Yan, L.-K.; Zhang, Y.-T.; Xu, M.-T.; Hayfron-Benjamin, E.; Su, Z.-M. On the origin of the relative stability of Wells–Dawson isomers: A DFT study of  $\alpha$ -,  $\beta$ -,  $\gamma$ -,  $\alpha^*$ -,  $\beta^*$ -, and  $\gamma^*$ -[(PO<sub>4</sub>)<sub>2</sub>W<sub>18</sub>O<sub>54</sub>]<sup>6-</sup> anions. *Inorg. Chem.* **2011**, *50*, 4967–4977. [[CrossRef](#)] [[PubMed](#)]

31. Baker, L.C.W.; Figgis, J.S. New fundamental type of inorganic complex: Hybrid between heteropoly and conventional coordination complexes. Possibilities for geometrical isomerisms in 11-, 12-, 17-, and 18-heteropoly derivatives. *J. Am. Chem. Soc.* **1970**, *92*, 3794–3797. [[CrossRef](#)]
32. Dawson, B. The structure of the 9(18)-heteropoly anion in potassium 9(18)-tungstophosphate,  $K_6(P_2W_{18}O_{62}) \cdot 14H_2O$ . *Acta Crystallogr.* **1953**, *6*, 113–126. [[CrossRef](#)]
33. Neubert, H.; Fuchs, J. Crystal structures and vibrational spectra of two isomers of octadecatungsto-diarsenate  $(NH_4)_6As_2W_{18}O_{62} \cdot nH_2O$ . *Z. Naturforsch.* **1987**, *42b*, 951–958. [[CrossRef](#)]
34. Contant, R.; Thouvenot, R. A reinvestigation of isomerism in the Dawson structure: Syntheses and  $^{183}W$  NMR structural characterization of three new polyoxotungstates  $[X_2W_{18}O_{62}]^{6-}$  ( $X = P^V, As^V$ ). *Inorg. Chim. Acta* **1993**, *212*, 41–50. [[CrossRef](#)]
35. Richardt, P.J.S.; Gable, R.W.; Bond, A.M.; Wedd, A.G. Synthesis and redox characterization of the polyoxo Anion,  $\gamma^*-[S_2W_{18}O_{62}]^{4-}$ : A unique fast oxidation pathway determines the characteristic reversible electrochemical behavior of polyoxometalate anions in acidic media. *Inorg. Chem.* **2001**, *40*, 703–709. [[CrossRef](#)] [[PubMed](#)]
36. Zhang, J.; Bond, A.M. Voltammetric reduction of  $\alpha$ - and  $\gamma^*-[S_2W_{18}O_{62}]^{4-}$  and  $\alpha$ -,  $\beta$ -, and  $\gamma$ - $[SiW_{12}O_{40}]^{4-}$ : Isomeric dependence of reversible potentials of polyoxometalate anions using data obtained by novel dissolution and conventional solution-phase processes. *Inorg. Chem.* **2004**, *43*, 8263–8271. [[CrossRef](#)] [[PubMed](#)]
37. Sun, Y.-X.; Zhang, Z.-B.; Sun, Q.; Xu, Y. Syntheses, characterization and catalytic properties of two new Wells–Dawson molybdosulfates. *Chin. J. Inorg. Chem.* **2011**, *27*, 556–560.
38. Brown, I.D.; Altermatt, D. Bond-valence parameters obtained from a systematic analysis of the Inorganic Crystal Structure Database. *Acta Crystallogr.* **1985**, *B41*, 244–247. [[CrossRef](#)]
39. Zonnevijlle, F.; Tourné, C.M.; Tourné, G.F. Preparation and Characterization of Iron(III)- and Rhodium(III)-Containing Heteropolytungstates. Identification of Novel Oxo-Bridged Iron(III) Dimers. *Inorg. Chem.* **1982**, *21*, 2751–2757. [[CrossRef](#)]
40. Tézé, A.; Hervé, G.  $\alpha$ -,  $\beta$ -, and  $\gamma$ -Dodecatungstosilicic acids: Isomers and related lacunary compounds. *Inorg. Synth.* **1990**, *27*, 85–96.
41. Sheldrick, G.M. A short history of SHELX. *Acta Crystallogr.* **2008**, *64*, 112–122. [[CrossRef](#)] [[PubMed](#)]



© 2016 by the authors; licensee MDPI, Basel, Switzerland. This article is an open access article distributed under the terms and conditions of the Creative Commons Attribution (CC-BY) license (<http://creativecommons.org/licenses/by/4.0/>).